Int. J. Adv. Res. Sci. Technol. Volume 4, Issue 2, 2015, pp.302-307.

IJARST

International Journal of Advanced Research in Science and Technology

journal homepage: www.ijarst.com

ISSN 2319 – 1783 (Print)
ISSN 2320 – 1126 (Online)

High energy Oxygen ion irradiation effects on thin films of $Sr[(Mg_{0.32}Co_{0.01})Nb_{0.67}]O_3$

Bhagwanti Bishnoi[1] and P.K. Mehta[2]*

[1]***Krishna Institute of Engineering and Technology, Department of Applied Sciences, Ghaziabad- 201 206 (U.P), India.***

[2]***Department of physics, Faculty of Science, The M. S. University of Baroda, Vadodara-390002, Gujarat, India***

****Corresponding Author's Email:** bhagwanti.bishnoi@kiet.edu*

A R T I C L E I N F O

Article history:
Received 02 Jan. 2015
Accepted 20 Jan. 2015
Available online 16 Feb. 2015

Keywords:
Thin Films, pulse laser deposition, dielectric properties, AFM, UV, Swift heavy ion irradiation.

PACS:
73.50. Rb, 81.15Fg, 61.80Jh, 77.22Ch 68.37.Ps

A B S T R A C T

Present paper gives detailed investigation of $Sr[(Mg_{0.32}Co_{0.01})\ Nb_{0.67}]O_3$ [SMCN] thin films deposited on ITO coated glass substrate using Pulse laser deposition technique. In order to probe the stability of SMCN under high energy ion irradiation, swift heavy ion (SHI) beam irradiation experiments are performed using 100MeV O^{7+} ion beams. The effect of irradiation on films, fluence of 1×10^{12} and 1×10^{13} ions/cm^2, are investigated by X- ray diffraction (XRD), UV-Vis spectroscopy, atomic force microscopy (AFM) and dielectric measurements. It reveals polycrystalline and uniform columnar growth in as- deposited films. Ion irradiation leads to partial amorphization as observed in AFM results. We have also observed drastic reduction in dielectric loss tangent (Tanδ) values. At 1×10^{13} fluence film shows very low values of tanδ~0.008 at room temperature. The temperature coefficient of dielectric constant (TCK) after irradiation has drastically fallen to 1/2 of its value in unirradiated film. Optimization of critical irradiation parameters may lead to its applicability in devices.

© 2015 International Journal of Advanced Research in Science and Technology (IJARST). All rights reserved.

Introduction:

The availability of thin-film based dielectrics/ferroelectrics has encouraged the integration of these materials with semiconductor circuits, and architecture. This combines the excellent properties of dielectric/ferroelectrics with micro machined silicon structures [1,2]. The materials studied so far include PZT, PLZT, PMN-PT, PFN, BST and SBT probed for its memory applications. Although lead based systems shows good ferroelectric properties but they suffer from severe fatigue problems [3]. An environmentally friendly barium, strontium, calcium or bismuth based layered systems are useful alternatives. In these systems strain is one of the important factors altering the dielectric properties, as it is directly coupled with the ionic polarization in a dielectric/ferroelectric [4-7]. The desired critical parameters are high dielectric constant, low temperature coefficient of dielectric constant, and low electrical loss in particular for dielectric materials based devices.

Irradiation of materials with swift heavy ions, such as the O^{7+} ion beam in the present case, dissipate their energy, partial or completely, in the medium leading to creation of defects as well as structural changes altering samples properties. High energy heavy ion beam loses their energy in a medium through two processes, namely, electronic loss (Se) and nuclear collisions (Sn).The latter process is the dominant mode of energy loss at low ion energies and peaks approximately at 1 keV/u. It is responsible for displacing atoms of the medium from their lattice positions. On the other hand the electronic energies loss is appreciable at higher ion energies and peaks approximately at 1 MeV/u. In this process the target atom is not displaced but only excited or ionized. However, it can also lead to displacement of lattice atoms in a cylindrical core along the ion path in insulating material either through the columbic explosion [8] or as thermal spike [9]. Along their latent tracks the material suffers partial amorphization. The irradiation also enhances the role of defects as the electrons/holes created by irradiation are violently separated and then gets trapped at the lattice point defects, stoichiometric defects, impurities and at grain boundaries. Further, the grain boundaries are known to offer high resistance to movement of these trapped charges. The trapped charges get pinned in domains and consequently modify material properties. Since the polycrystalline thin films contain small crystalline grains and smaller domains, which may contribute to larger number of traps per unit area [10]. This in turn leads to the enhanced pinning of charges in domains

and subsequent noticeable alteration of thin films ferroelectric/dielectric properties.

There are very limited reports on the study of high energy swift heavy ion irradiation (SHI) effects on ferroelectric thin films. It is reported that Strontium Barium Titanate (SBT) thin film based memories when exposed to xenon ions with a fluence of 1.5×10^7 ions/cm^2 did not lose any data [11]. Whereas X-ray and γ-ray irradiation of PZT thin films showed degradation of the ferroelectric properties. [10,12]. The neutron irradiation of PZT, lanthanum doped lead zirconate titanate (PLZT) and lead zirconate (PZ) thin films also showed considerable degradation in the ferroelectric properties [13]. Further, decrease in phase transition temperature (Tc) was observed on neutron irradiation for the anti-ferroelectric PZ films [13] and PLZT ceramics [14]. This lowering of the Tc after irradiation was attributed to the destruction of ferroelectric ordering and the breaking of the macro polar domain into micro polar domains, reducing the size of polar region.

In the present case we have used 100 MeV O^{7+} ion beams on SMCN thin films. The electronic energy loss (*Se*), nuclear energy loss (*Sn*), and the range of the ion Rp are calculated by using standard SRIM simulation program and tabulated in Table 1. From the table I it is clearly evident that *Sn* is very much less than that of Se and the range is much larger than that of the film's thickness (0.25 μm) and hence the energy are not going to be implanted in the films. High values of Se compared with the *Sn* indicate that the energy dissipated in the film is mainly through the electronic excitation and ionization. As, the film thickness is small compared with the range, the Se has constant value throughout the films. Hence the irradiation effects are expected to be produced uniformly throughout the thickness of the film.

The search for appropriate material in thin films form for device applications led us to probe the Oxygen ion irradiation effects on $Sr[(Mg_{0.32}Co_{.01})\ Nb_{0.67}]O_3$ [SMCN] thin films coated on ITO substrates using Pulsed Laser Deposition (PLD). We observed reduction in grain size and marginal increased lattice strain in the film on irradiation. Although it has led to reduction in dielectric constant but it has simultaneously led to reduction of dielectric loss to a greater extent. The resultant enhancement of Q factor (1/tanδ) is likely to benefit its future applications.

Experimental Details:

SMCN target was made by conventional solid-state reaction technique in air. In the first stage, $[(Mg_{0.32}Co_{0.01})Nb_{0.67}]O_3$ precursor phase was produced from MgO (≥99%), Co_3O_4 (≥99%), Nb_2O_5 (≥99%) powders taken in stoichiometric proportions. The powders were then mixed homogenously and pressed lightly into pellets and calcined at 900°C for 6hrs. After the initial precursor heating cycles, a stoichiometric amount of $SrCo_3$, is added, intimately mixed, and calcined at 900°C overnight to decompose the carbonate. Intermediate grindings and repelletization were performed with multiple heating cycles in the temperatures range of 900°C to 1200°C. The bulk target was then mounted in a deposition chamber which was subsequently evacuated to a base pressure of $\sim 5 \times 10^{-5}$ Torr. A pulsed KrF (wavelength λ = 248 nm), excimer laser was used for ablation (repetition rate of 10 Hz and energy density of 220 mJ/cm^2). Laser radiation was focused onto the SMCN target in the chamber. Prior to the mounting the ITO coated glass substrate into the deposition chamber, they were degreased ultrasonically, first in CCl_4, then in acetone and finally in methanol. These substrates were mounted parallel to the target at a distance of 4cm and heated upto ~300°C. Oxygen introduced into the chamber during deposition was maintained at a pressure of 200 mTorr during deposition. The thickness of all the deposited films is around ~250 nm, which we measured by stylus profilometer. The x-ray diffraction data were used to confirm the formation of a single phase compound.

The well characterized films were irradiated at room temperature with 100 MeV O^{7+} ion beams with different fluences of 1×10^{12}, 1×10^{13} ions/cm^2 using a 15UD tandem accelerator at the Inter University Accelerator Centre (IUAC), previously called as Nuclear Science Centre (NSC), New Delhi, India. The beam current was kept around 0.5-1 pnA for O^{7+}, to avoid heating. The ion beam was focused to a spot of ~1 mm diameter and scanned over the entire area of the thin film using a magnetic scanner. The ion beam fluence was measured by integrating the ion charge on the sample ladder, which was insulated from the chamber. The SMCN thin films were characterized by Shizmadu X-ray diffractometer 6000 with (λ= 1.5402Å). The thin film morphology on a wide range of scan lengths (500 μm to 1 μm) was investigated by Atomic Force Microscopy (AFM) using Nan scope-E from Digital Instruments, USA. Dielectric constant measurement were measured using a Agilent 4285A (LCR) bridge which has a frequency range of 75 KHz to 30 MHz and operated in the temperature range 100 K to 450 K. UV-Vis spectra were recorded using a Hitachi U-3300 spectrophotometer.

Results:

XRD study:

To check the crystalline nature and phases present in the as- deposited and irradiated thin films, systematic, XRD measurement were performed and presented in the Figure 1.

It shows the XRD pattern of SMCN bulk, as-deposited, irradiated SMCN thin film, 1×10^{12} ions/cm^2 irradiated SMCN thin film, and 1×10^{13} ions/cm^2 irradiated SMCN thin film, respectively. The comparison of XRD pattern of bulk material with films confirms the single phase of the films. The observed

XRD peak, ~ 30.3° (bulk), appeared to be shifted lit bit towards the higher angles, in as- deposited and irradiated SMCN thin films. On irradiation the intensity of the peak is reduced at the highest fluence which is likely to be due to the partial amorphization on irradiation.

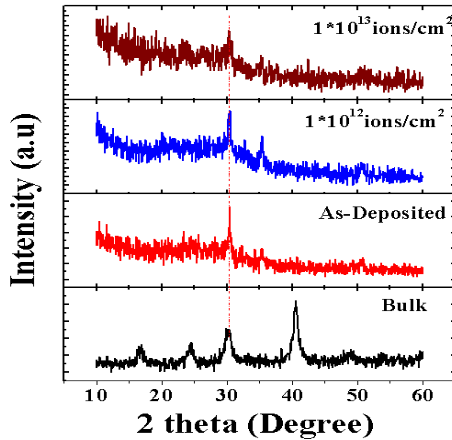

Figure: 1. SMCN X-ray diffraction pattern of bulk, as-deposited, irradiated films with different fluence

AFM study:

Besides the structural modifications, the SHI irradiation is also known to tailor surface microstructures of the film material. Therefore, to further probe the surface microstructures of as-deposited and irradiated SMCN thin films, systematic, AFM measurements were perform on the samples. Figure.2(a)-(b) show the two dimensional (2D) images while Figure 2(c)-(d) show the three dimensional (3D) views of corresponding 2D images of as- deposited, and 1×10^{13} ion/cm^2 irradiated SMCN thin films, respectively. It is clear from the Figure 2(a) and (c) that as- deposited SMCN thin films shows smaller and coarse grains. The calculated root mean square (RMS) roughness of the as- deposited film is ~5.341 nm. Here we have shown the result of highest fluence (1×10^{13}) ions/cm2. The irradiated sample shows that the grains are completely agglomerated/cobbled at highest fluence. The RMS roughness of the film at the highest fluence is found to be ~36.74nm. This shows that grains have completely amorphized at highest fluence and the film surface shows pinning (Columnar) tracks have been formed.

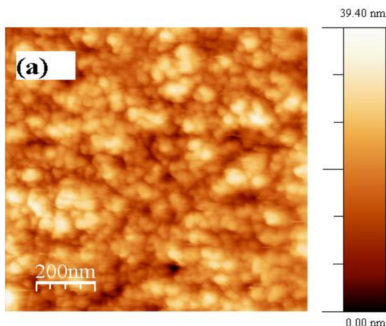

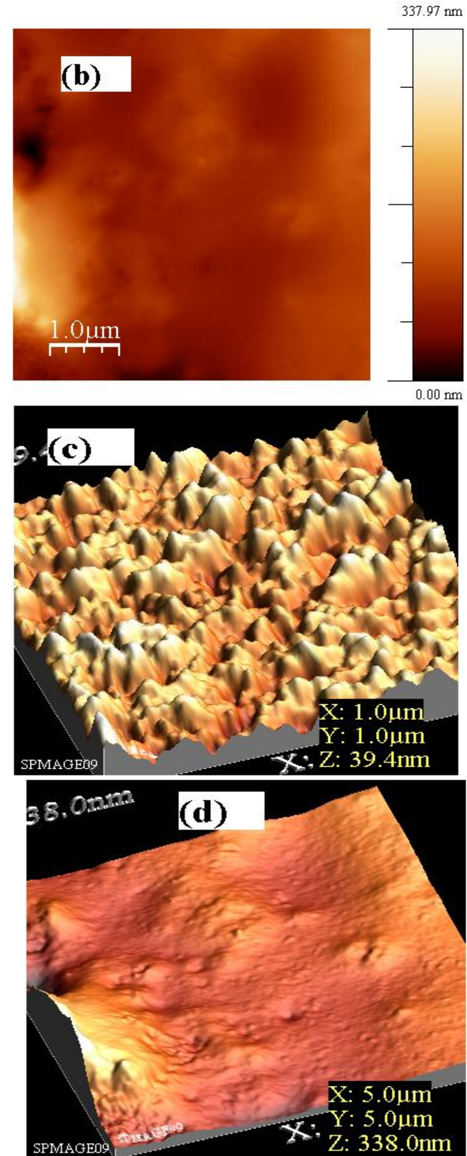

Figure: 2. AFM micrographs of as- deposited and irradiated SMCN thin films.

Dielectric Measurement:

Figure: 3(a) shows the temperature dependence of the dielectric constant of as- deposited, and 100 MeV O^{7+} irradiated samples at two different fluences from 100 KHz - 1.1 MHz frequencies. Earlier, we have reported that the un-irradiated films shows abrupt rise in the magnitude of dielectric constant compared to that of bulk [15]. This is suggested to be due to the effects of strain during the deposition rather than lattice mis-match. On irradiating the films with O^{7+} ion beam we here find decrease in the magnitude of dielectric constant (by a factor of 1/10). This observed fall in values could be due to the defects created in the films in the form of partial amorphization along the latent tracks. We observed similar effects in polar dielectric materials like $Ba[(Mg_{0.32}Co_{.01})\ Nb_{0.67}]O_3$ (BMCN) [16]. The reason behind the decrease in dielectric constant in films is the alteration in lattice strain as well as the

amorphization induced depolarization. It should be noted that BMCN being a polar material shows before and after irradiation nearly linear temperature dependence of ε' and tanδ. On the other hand, non-polar system like, SMCN exhibit peak formation in ε' and tanδ, a signature of relaxor properties.

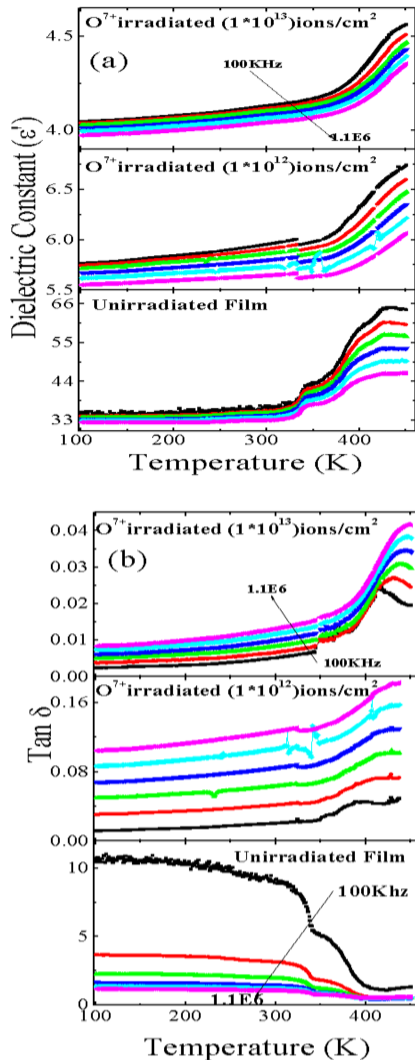

Figure: 3. the temperature dependence of (a) dielectric constant and (b) dielectric loss (Tanδ) of as- deposited and O^{7+} irradiated films with different fluence.

Figure: 3 (b) shows the temperature dependence of the dielectric loss (tanδ) of as- deposited and 100 MeV O^{7+} ion beam irradiated samples at two different fluence with frequencies varying from 100 KHz -1.1E6. The unirradiated film shows the dielectric loss to be as high as 10 at 100 KHz but reduces with increase in frequencies and temperature. On irradiating it with O^{7+} ion beam of fluence 1×10^{12} ions/cm^2, we observe a considerable amount of reduction in the loss values (nearly by a factor of 1/100). On further increasing the fluence to the order of 1×10^{13} ions/cm^2 the loss is reduced to a still lower value of 0.008 at (300 K) and at highest frequencies. A closer look at Figure 3(b) reveal that variations in dielectric loss as a function of temperature and frequency is completely reversed on irradiation in comparison to un-irradiated state. Above trends of dielectric parameter variations suggest that controlled irradiation by 100 MeV O^{7+} ion beam could help in controlling fall in dielectric constant along with maintaining drastic fall in the dielectric loss parameter which will enhance its applicability in microwave and memory devices. The dielectric parameters with the change in fluence are tabulated in Table I.

Table: I. Dielectric Properties of $Sr[(Mg_{0.32}Co_{0.01})Nb_{0.67}]O_3$ [SMCN] thin films at 500 KHz

Fluence	Dielectric Constant (ε')	Dielectric Loss (Tan δ)
As- Deposited	35.08	1.95
O^{7+}irradiated (1×10^{12})ions/cm^2	5.85	0.0633
O^{7+}irradiated (1×10^{13})ions/cm^2	4.10	0.0083

It is to be noted here that in comparison to earlier reports on other ABO_3 based compounds [11-14], we find that irradiating the SMCN thin films with 100 MeV O^{7+} ion beam though reduced the dielectric constant by a factor of 101 along with marginally increased Tc but helped to reduce dielectric loss 10-2 times. Further, it also exhibited improvement compared our observations on BMCN films [16], which showed enhancement in dielectric loss on O^{7+} ion beam irradiation. Earlier we did report improvement in dielectric properties on O ion beam irradiation in $Ba(Co_{1/3}Nb_{2/3})O_3$ thin films [17].

Figure 4 shows frequency dependence of dielectric constant and dielectric loss (tanδ) at room temperature. Both these parameters (ε' and tanδ) decreases for films after irradiation with no significant frequency dependent dispersion. Contrary to this un-irradiated film showed drastic fall in tanδ and ε' at high frequencies.

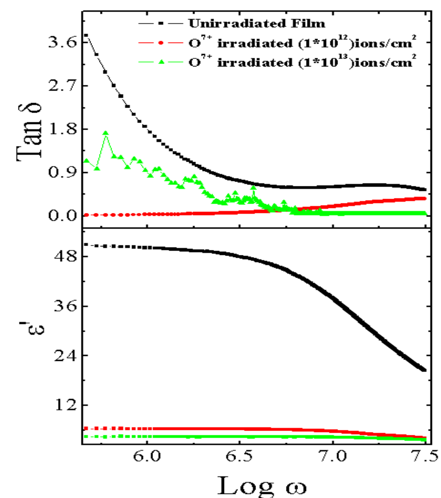

Figure: 4. Variation of dielectric constant (ε') and dielectric loss (Tanδ) at room temperature for as-deposited and irradiated films with different fluences.

UV- Study:

To understand the optical properties of as-deposited and irradiated in SMCN thin films, UV-Visible absorption spectroscopy measurements have been performed. The optical band gap has been calculated by Tauc's procedure of plotting the $(\alpha h\nu)^2$ vs hν and shown in Figure 5. The optical band gap of as-deposited film is 2.29 eV, which is less than the band gap of the SMCN bulk materials (2.89 eV).

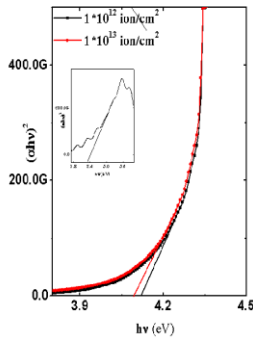

Figure: 5. UV-visible absorption spectra of as-deposited (inset) and 100 MeV O7+ ion beam irradiated SMCN thin films.

The inset in Figure 5 shows the band gap of as-deposited film. In the irradiated films the optical band gap is found to be higher than the as- deposited film which shows significant shift in absorption edge. The calculated energy band gap of the 1×10^{12} and 1×10^{13} ion/cm^2 irradiated sample are 4.12, and 4.09 eV, respectively. The decrease in the band gap of the irradiated sample can arises due to agglomeration of the sample. Thus the SHI irradiation helps in tailoring the optical band gap of the oxide films by creating defects/ agglomeration in the films.

Discussion on the possible mechanisms:

Ion irradiation induced structural modification probed through our XRD, AFM, and Dielectric measurements could be understood by knowing the energy transfer processes of energetic ions and rising of local temperature in the film material. The electronic energy loss (*Se*), nuclear energy loss (*Sn*) and range of 100 MeV O^{7+} ions in the SMCN target were calculated using the stopping and range of ions in matter (SRIM) software [18]. Figure 6(a) shows the *Se* and *Sn* profile of O ion beam in SMCN. In the Figure 6(b), we have plotted depth vs. Se and Sn of O^{7+} ion beam in SMCN matrix. From the Fig. 6 it is clear that most the energy is lost in SMCN material by electronic energy loss process and nuclear energy loss process dominant in the low energy regime. The range of 100 MeV O^{7+} ions in SMCN target is about 109μm, thus all the atoms are expected to pass through the film thickness (200 nm) deep into the substrate. In order to explain the SHI irradiation effects on the material modifications there are two models (i) Coulomb explosion and (ii) Thermal spike model (19-21,10). In Coulomb explosion model the relaxation of the localized excess of energy occurs via radial impulse of atoms lying in the surrounding area of the ion path within the 10-15s [19-20]. In this process a highly positive charged zone of target material explodes due to coulomb repulsion before electrical neutrality is achieved. In the thermal spike model, energetic ions deposit their energy to the electronic subsystem of the target atoms and lead to rising of the local temperature of the material via electron-phonon coupling. As a result of electronic excitation and effective electron-phonon coupling, a cylindrical region around the ion track become fluid in the sense that thermally induced shear stress/strain may relax in this region [22] and formation of nano-crystalline phases may also take place [23]. Along the ion path crystalline to non-crystalline phase transformation is possible provided that the local temperature of the material, during thermal spike formation, is greater than the phase transition temperature [24].

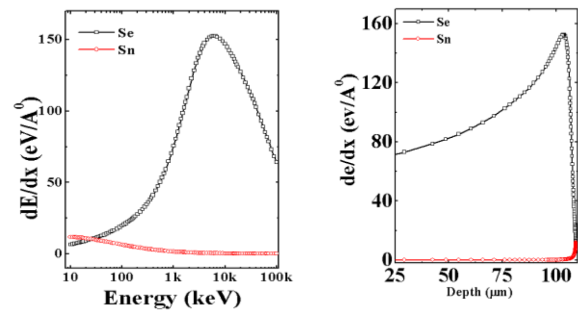

Figure: 6. The *Se* and *Sn* profile of O^{7+} ion beam in SMCN and Depth vs. *Se* and *Sn* of the O^{7+} ion beam in SMCN

Conclusion:

The SMCN thin films on ITO coated glass substrates, were successfully deposited by Pulsed laser deposition technique and irradiated with 100 MeV O^{7+} ion beams. The AFM images show that the RMS roughness is increased and surface microstructures have been engineered with varying irradiation fluence. Irradiation by 100 MeV O ion beam with fluence upto 1×10^{13} ions/cm^2 though reduces the dielectric constant by a small factor of 101 but observed advantages are drastic reduction in dielectric loss, (by from 10 to 10^{-2} or less). These are much desirable sign for its future applications as microwave resonator and filter. Further optimization of ion irradiation parameters could help in stabilizing dielectric constant values along with drastic reduction in the dielectric loss, significantly enhancing films applicability as devices.

Acknowledgement:

One of the authors Dr Bhagwanti Bishnoi is very much thankful to the Inter University Accelerator centre (IUAC) New Delhi for providing financial support under the project UFUP-41315 and for

providing irradiation and measurement facility. The author (Dr Bhagwanti Bishnoi) is also thankful to the Director, KIET, GZB and Dr C M Batra for their immense help in various ways.

References:

1. Basavaraj Angadi, P Victor, V M Jali, M T Lagare, Ravi Kumar, S. B. Krupanidhi, *Mat. Sci. Engg. B* 2003, 100, 93-101.
2. J Petzelt, T Ostapchuk, *J Opto electron Adv Mater*, 2003, 5, 725.
3. Basavaraj Angadi, P Victor, V M Jali, M T Lagare, Ravi Kumar, S. B. Krupanidhi, *Thin Solid Films* 2003, 434, 40-48.
4. W J Merz *Phys Rev*, 1950, 78, 52-54.
5. C J Slater, *Phys Rev*, 1950, 78, 748-761.
6. P W Forsbergh, Jr *Phys Rev*, 1954, 93, 686-692.
7. G A Samara, A. A. Giardini *Phys Rev*, 1965, 140, A954-A957.
8. D Lesueur, A Dunlop, *Rad. Eff. Def. Sol*, 1993, 126, 163-172.
9. G Szenes, *Phys Rev B*, 1995, 51, 8026-8029
10. Coic Y M, O Musseau, L J Leray, *IEEE Trans Nucl Sci,* 1995, 41,495.
11. M J Benedetto, F G Derbenwick, D J Cuchiaro JD, *IEEE Trans Nucl Sci*, 1999, 46, 1421.
12. C S Lee, G Teowee, D R Schrimpf, P D Birnie, R D Uhlmann, F K Galloway, *IEEE Trans Nucl Sci*, 1992, 39,2036.
13. R Bittner, K Humer, H. W. Weber, M Tyunina, L Cakare, A Sternberg, D V Kulkov, Y V Trushin, *Integrated Ferroelectrics* 2001, 37,275-283.
14. A Sternberg, A Spule, L Shebanovs, E Birks, W H Weber, H Klima, F Sauerzopf, *Key Eng Mater,* 1997, 132,1096.
15. P K Mehta, Bhagwati Bishnoi, Ravi Kumar, R J Choudhary, D M Phase, *Solid State Phenomena,* 2009, 155,145-149.
16. N V Patel, Bhagwati Bishnoi, P K Mehta, Ravi Kumar, R J Choudhary, D.M. Phase, V Ganesan, C J Panchal, *J Nano Elect Phys,* 2012, 4, 04001-04004.
17. Bhagwati Bishnoi, P K Mehta, C J Panchal, M S Desai, Ravi Kumar, V Ganesan, *Mat Chem Phys*, 2011, 126,660-664
18. J. F. Ziegler, M. D. Ziegler, J. P. Biersack, Stopping and Ranges of Ions in Matter, SRIM code 2008 (www.srim.org)
19. M. Toulemonde and C. Dufour R. Kelly, *Phys. Rev. B* 1992, 46, 14362-14369
20. R. L. Fleischer, P. B. Price, R. M. Walker, *J. Appl. Phys,* 1965, 36, 3645.
21. E. M. Bringa, R. E. Johnson, *Phys, Rev. Lett*, 2002, 88,165501-165504.
22. T Mohanty, P. V. Satyam, D. Kanjilal, *J. Nanosci. Nanotechnology.* 2006, 6, 2554.
23. M. Varshney, A. Sharma, K.D. Verma, R. Kumar, *Nucl. Instr. Meth. Phys. Res. B269,* 2011, 250, 2786-2791.
24. H. Rath, P. Das, T. Som, P. V. Satyam, U. P. Singh, P. K. Kularia, D. Kanjilal, D. K. Avasthi, N. C. Mishra, *J. Appl. Phys.* 2009, 105, 074311.